

Revised Version

Submitted to Analytical Chemistry

Hydrodynamic Chromatography On-line with Single Particle -
Inductively Coupled Plasma – Mass Spectrometry for Ultratrace
Detection of Metal-Containing Nanoparticles

Spiros A. Pergantis^{a,b,}, Tammy L. Jones-Lepp^a, Edward M. Heithmar^a*

^aU.S. Environmental Protection Agency, National Exposure Research Laboratory, Environmental Sciences
Division, 944 E. Harmon Avenue, Las Vegas, NV 89119, USA

^bEnvironmental Chemical Processes Laboratory, Department of Chemistry, University of Crete, Voutes Campus,
Heraklion, 71003, Greece

* Author for correspondence: spergantis@chemistry.uoc.gr

ABSTRACT

Nanoparticle (NP) determination has recently gained considerable interest since a growing number of engineered NPs are being used in commercial products. As a result, their potential to enter the environment and biological systems is increasing. In this study we report on the development of a hyphenated analytical technique for the detection and characterization of metal-containing NPs, i.e. their metal mass fraction, size and number concentration. Hydrodynamic chromatography (HDC), suitable for sizing NPs within the range of 5 to 300 nm, was coupled on-line to inductively coupled plasma mass spectrometry (ICPMS), providing for an extremely selective and sensitive analytical tool for the detection of NPs. However, a serious drawback when operating the ICPMS in its conventional mode is that it does not provide data regarding NP number concentrations, and; thus, any information about the metal mass fraction of individual NPs. To address this limitation, we developed single particle (SP) ICPMS coupled on-line HDC as an analytical approach suitable for simultaneously determining NP size, NP number concentration and NP metal content. Gold (Au) NPs of various sizes were used as the model system. To achieve such characterization metrics, three calibrations were required and used to convert ICPMS signal spikes into NPs injected, NP retention time on the HDC column to NP size, and ions detected per signal spike or per NP to metal content in each NP. Two calibration experiments were required in order to make all three calibrations. Also, contour plots were constructed in order to provide for a convenient and most informative viewing of this data. An example of this novel analytical approach was demonstrated for the analysis of Au-NPs that had been spiked into drinking water at the ng Au L^{-1} level. The described technique gave limits of detection for 60 nm Au-NPs of approximately 2.2 ng Au L^{-1} or expressed in terms of NP number concentrations $600 \text{ Au-NPs mL}^{-1}$. These were obtained while the 60 nm NPs exhibited a retention time of 771 sec at a mobile phase flow rate of 1 mL min^{-1} .

INTRODUCTION

Because of their unique physicochemical properties, nanomaterials are finding use in an increasing number of consumer products.^{1,2,3} Silver (Ag) nanoparticles (NPs) have already been introduced in over 100 products, ranging from nutritional supplements, personal care products, biocide coatings, clothing, toys as well as dispersed biocides in washing machines.^{4,5,6,7} Other nanomaterials, including TiO₂, ZnO, Au, CeO, carbon nanotubes and fullerenes, are found in a wide range of consumer products.⁷ Recent reports show over 1300 consumer products contain engineered nanomaterials.⁷ This, of course, is very attractive to consumers as products with unique properties and improved quality are continuously becoming available. In fact, such developments are hinting that a nanotechnology based revolution is rapidly approaching.

The increasing use of nanomaterials, however, is generating urgent and important questions regarding their fate and potential effect on the environment and living organisms.^{8,9} To address such questions numerous analytical techniques and methods have been developed and applied to provide information on a wide range of nanomaterial characterization metrics. More specifically, size distribution as it relates to nanoparticle (NP) diameter is measured using microscopic techniques [i.e. scanning electron microscopy (SEM), transmission electron microscopy (TEM), and atomic force microscopy (AFM)],^{10,11,12} dynamic and static light scattering techniques (DLS and SLS),^{13,14} NP tracking analysis,¹⁵ and separation techniques including field-flow fraction (FFF),¹⁶ capillary electrophoresis,¹⁷ ion mobility spectrometry¹⁸ and hydrodynamic chromatography (HDC)¹⁹. Another size distribution characteristic, related to NP mass, and not NP diameter, can be measured using sedimentation FFF.²⁰ Additional relevant characterization metrics include nanomaterial surface properties such as specific surface area²¹ and surface charge²². Nanomaterial or NP shape measurements are important in many cases and can be carried out using SEM, TEM, AFM, DLS and FFF.²³ Ultimately, however, NP concentrations need to be determined in a variety of sample types, and even though a strong analytical arsenal has been developed for their characterization, critical limitations still exist. Most importantly, methods are needed for the detection and characterization of NPs in environmental samples, in which

case NPs, if present, are at extremely low concentrations in complex sample matrices. This necessitates extensive sample preparation prior to the use of existing analytical techniques, e.g. matrix removal and/or NP preconcentration. However, this is not without difficulty as sample pretreatment may cause formation of NP artifacts as a result of aggregation and/or losses. Thus it is imperative to develop analytical techniques that are suitable for addressing these critical limitations in order to detect NPs in environmental and biological samples, at concentrations that are relevant to those specific sample types.

In an effort to achieve this, Tiede *et al.* have recently demonstrated the development¹⁹ and application²⁴ of hydrodynamic chromatography (HDC) on-line with inductively coupled plasma – mass spectrometry (ICPMS) for detecting and studying the behavior of metal-containing engineered NP in complex environmental matrices. It was claimed that the utilized HDC column is suitable for sizing NPs within the range of 5 - 300 nm. Other attractive features include rapid analysis time (typically <10 min) and minimum requirement for sample pre-treatment. These features, in combination with the selectivity and sensitivity of the ICPMS detector, make HDC – ICPMS a powerful and promising technique for investigating the fate of a significant range of NP types. In their paper, Tiede *et al.*¹⁹ concluded that “this approach offers a robust, novel, complementary technique, suitable for the routine size and elemental characterization of inorganic engineered NPs in environmental fate and ecotoxicity studies”.

However, this promising approach still has disadvantages that require further investigation and improvement. In particular, even though hyphenated methods, like HDC – ICPMS, are suitable for providing both metal content and size distribution information of the analyzed NPs in relatively complex samples, they have not been demonstrated to provide NP number concentration information. This is a serious drawback as the approach cannot distinguish between a high concentration of NPs, each containing a small fraction of metal, from a low concentration of the same sized NPs each containing a high metal fraction. For example, Au NPs with a 40 nm diameter cannot be distinguished from 40 nm organic NPs each containing traces of Au. In fact, no information regarding NP number concentration can be obtained, as the approach only allows for the determination of total metal concentration and particle size.

To address this drawback, we have investigated the use of single particle-ICPMS (SP-ICPMS) on-line with HDC. The use of SP-ICPMS, without any on-line chromatographic coupling, has recently been demonstrated to be suitable for simultaneously determining the concentration of metal-containing NPs and measuring the metal mass in individual NPs.^{25,26,27,28,29,30,31} However, unless coupled with size separation, it is not suitable for determining the size of NPs unless their element composition is known. A related technique was originally developed to characterize airborne particulates,^{32,33} and was later adapted for characterizing zirconia colloids,²⁵ thorium oxide,²⁶ and Au particles²⁷. Recently, the technique was applied to characterize Ag NPs in municipal waste water,²⁸ and preliminary results of the technique coupled with flow-FFF have been presented³⁴. Also recently, SP-ICPMS was used to detect Au-NPs collected from an ion mobility spectrometer.³⁵

In addition, in the present study, we have evaluated the capabilities of SP-ICPMS to provide improved sensitivity and limits of detection (LODs) when coupled on-line with HDC. In fact, Tiede *et al.*¹⁹ while presenting chromatograms of NP solutions with mg L⁻¹ metal concentrations, reported LODs of a few µg Au L⁻¹, thus not addressing the need to detect NPs at their anticipated ng L⁻¹ concentration level. To develop HDC – SP-ICPMS we have used Au NPs as the model system.

Experimental

Materials

Gold (Au) nanoparticles of several different sizes were used. Glass ampoules (5 mL) containing citrate-stabilized Au nanoparticles in aqueous suspension, having nominal diameters of 30 and 60 nm, were obtained from the National Institute of Standards & Technology (NIST). These are labeled by NIST as Reference Materials 8012 and 8013, respectively. Each Reference Material (RM) is provided with a Certificate of Investigation providing particle size (diameter) measurements, obtained using a series of independent analytical techniques, i.e. atomic force microscopy (AFM), scanning electron microscopy (SEM), transmission electron microscopy (TEM), electrospray - differential mobility analysis (ES-DMA), dynamic light scattering (DLS) and small-angle x-ray scattering (SAXS). NIST

RM 8013³⁶ is reported to have a Au mass fraction of $51.86 \pm 0.64 \mu\text{g g}^{-1}$, with a nominal diameter of 60 nm. The average diameter calculated by taking into account all measurements reported in the NIST 8013 certificate of investigation is 55.4 nm. NIST RM 8012³⁷ has a Au mass fraction of $48.17 \pm 0.33 \mu\text{g g}^{-1}$, and a nominal diameter of 30 nm. In this case, the average diameter calculated by taking into account all measurements reported in the NIST 8012 certificate of investigation is 26.8 nm.

Aqueous suspensions of citrate-stabilized Au NPs with a nominal size of 80 and 100 nm used in this study were obtained from Corpuscular (Microspheres-Nanospheres, Cold Spring, New York, USA).

Mobile Phase

A mobile phase consisting of 10 mM sodium dodecyl sulfate (SDS) solution adjusted to pH 11 was used throughout this study. The mobile phase was delivered at 1.0 or 1.6 mL min⁻¹.

Instrumentation and System Configuration

ICP-MS analyses were performed on a 7500ce (Agilent, Santa Clara, CA), with an upgraded 7500cx lens system. HDC-SP-ICPMS experiments were conducted using a hydrodynamic chromatography column (5-300 nm size range, Polymer Laboratories, Shropshire, UK) with a 100DM syringe pump (ISCO, Lincoln, NE). Samples were introduced via a 100 μL loop on a Rheodyne injection valve. Column effluent was introduced directly into a V-groove nebulizer situated on a double pass Scott spray chamber.

Data analysis was conducted using Excel spreadsheet (Microsoft) and Origin 8.5 (OriginLab) software.

Results and Discussion

Switching from HDC - conventional mode-ICPMS to HDC – SP-ICPMS for Au-NP Detection

The coupling of HDC on-line with conventional ICPMS and its application to investigate the behavior of NPs spiked into environmental matrices has recently been reported.^{19,24} In these studies the hyphenated technique was demonstrated to offer several advantages for detecting and studying NPs in environmental matrices. However, some critical limitations remain, most notably the technique's

inability to determine NP number concentration in the analyzed sample, i.e. number of NPs per sample volume. In addition, it remains to be demonstrated if the technique has the required sensitivity to provide limits of detection in the low ng metal L⁻¹ of sample (ppt) concentration level, as well as being suitable for detecting as low as a few hundred NPs in each injected sample. Thus, such analytical capabilities must be further developed, if the technique is to be of practical use for NP analyses.

Typically, when operating various types of liquid chromatography on-line with ICPMS for metal speciation analysis, ICPMS detector dwell times range from 100 - 500 ms for each isotope monitored. Such dwell times allow for the recording of a sufficient number of data points across a 20 to 60 s chromatographic peak and provide adequate signal-to-noise ratios for most metal speciation applications requiring detection at the $\mu\text{g L}^{-1}$ concentration level. We refer to such monitoring conditions as conventional mode – ICPMS. When used on-line with HDC to detect Au-NPs, conventional mode demonstrates some critical limitations. More specifically, when using HDC – ICPMS with a detector dwell time of 200 ms to monitor a single isotope, i.e. m/z 197 for Au, for the analysis of two solutions containing 30 nm or 200 nm Au NPs, the two superimposed chromatograms shown in **Figure 1** were obtained. First of all, from these chromatograms it is observed that the resolution of HDC is not sufficient to completely separate these two different sized Au-NPs. This is to be expected as HDC is a relatively low resolution separation technique. Nevertheless, the recorded chromatographic peaks, i.e. their peak area, give us information about the amount of Au present in the injected sample. In addition, the observed NP retention time (t_R) provides information about the size of the detected NPs, as elution in HDC depends only on NP size.³⁸ However, because we do not have information about NP number concentration, the size information in combination with the Au concentration does not provide further insight into the Au mass fraction of the NPs. Thus, important NP characterization metrics, i.e. NP number concentrations and their Au mass fraction, escape determination when using conventional mode-ICPMS.

In **Figure 1** it is also observed that the larger 200 nm Au NPs afford a chromatographic peak profile with numerous signal spikes superimposed upon it. In contrast, this is not observed for the smaller 30

nm Au NP chromatographic peak. The occurrence of signal spikes can be explained by the fact that when the larger 200 nm NPs atomize within the plasma each NP produces a significantly greater number of Au ions in the resulting “ion cloud” than do the 30 nm Au NPs. Therefore even a slight variation in the number of Au NPs entering the plasma per dwell time will produce substantial intensity variations, i.e. resulting in the observed spiking. Larger NPs are expected to produce larger signal spikes. Because NP-containing solutions are suspensions of solids in liquid, the occurrence of variations in the number of NP entering the plasma per dwell time cannot be avoided.

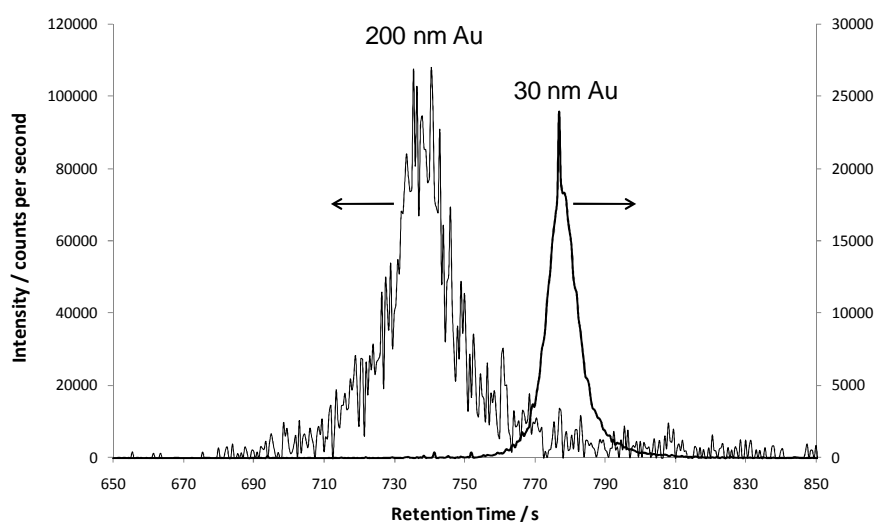


Figure 1. Superimposed HDC – conventional mode – ICPMS chromatograms for solutions containing 200 nm and 30 nm Au NPs, at 400 ng Au mL⁻¹ and 50 ng Au mL⁻¹, respectively. Acquired using a 200 ms dwell time for m/z 197, and a mobile phase flow rate of 1 mL min⁻¹.

To overcome such limitations and be able to detect individual NPs as they elute from the HDC column, we switched from conventional ICPMS to SP-ICPMS. For the latter mode of detection, the dwell time is set so that only a single NP is detected per dwell time by the ICPMS. This is possible by injecting sufficiently dilute samples, so that when the NPs elute from the column and the eluent is nebulized it produces an aerosol in which only a small fraction of aerosol droplets contain single Au-NPs, with the remaining droplets being void of Au-NPs. The ICPMS can detect a single Au-NP because as the particle travels through the plasma it is atomized and to some extent its atoms are ionized. Each plume of ions or the “ion cloud” enters the mass spectrometer over a period of approximately 0.5 ms.^{39,40} To capture and record the signal event from this discrete plume of ions, it is necessary to use

short detector dwell times. A dwell time of 10 ms was used in the present study, as this was the lowest the instrument would efficiently allow for. Similar dwell times have been used in several other SP-ICPMS studies.^{26, 31, 41} As a result, each discrete ion plume originating from a single NP is expected to give rise to a signal spike, the intensity of which is proportional to the mass of Au in the detected NP. However, if shorter dwell times were possible this would reduce the chance of detecting multiple NPs per dwell time. Also, shorter dwell times are expected to allow for the SP-ICPMS detection of greater NP number concentrations, this being especially important for the analysis of NP mixtures.

A typical HDC – SP-ICPMS chromatogram is presented in **Figure 2a**, in which signal spikes originating from 60 nm Au NPs, at a concentration of 50 ng Au L⁻¹, are observed. We refer to the

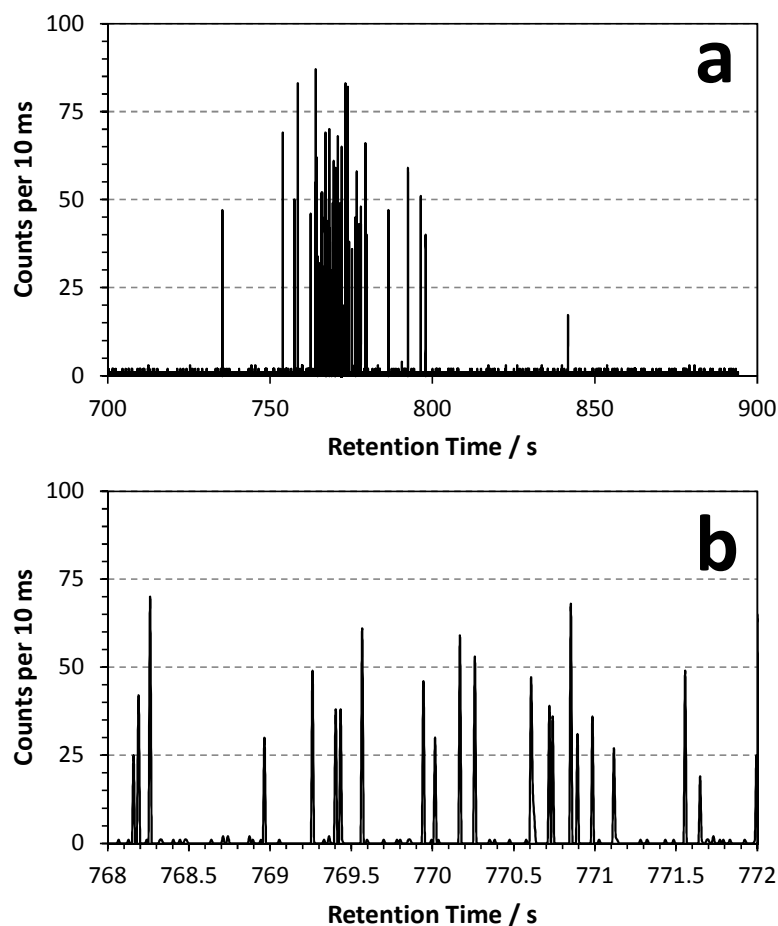


Figure 2 Spike-chromatogram of 60 nm Au NPs obtained using HDC – spICPMS at a mobile phase flow rate of 1 mL min⁻¹ (a). The solution injected had a concentration of 50 ng Au L⁻¹ or 5 pg of Au. Also presented is a 4 s zoom window of the recorded signal spikes (b).

resulting chromatogram, which is relatively unique in appearance, as a “spike-chromatogram”. The

information that can be extracted from such a spike-chromatogram is informative for NP characterization. To better observe the recorded signal spikes a 4 s time window of the spike-chromatogram is presented in **Figure 2b**. In this particular analysis, 54 signal spikes were counted, i.e. 54 NPs were detected. Their average intensity was 50 ions detected per NP, with a standard deviation of

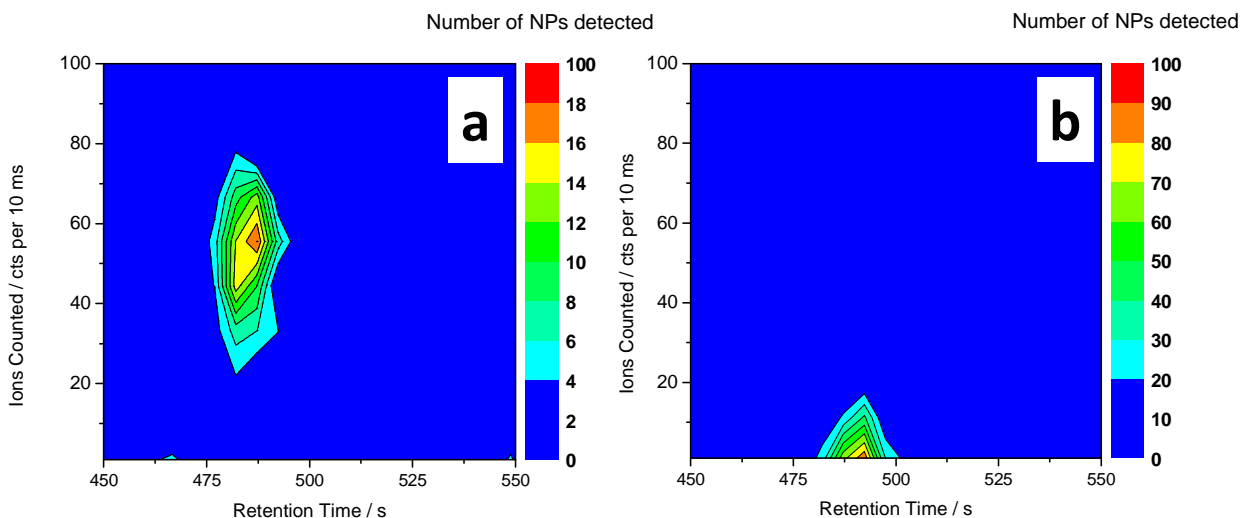


Figure 3 Contour plots obtained from the HDC – spICPMS analysis of Au-NPs having diameters of: (a) 60 nm (200 ng Au L^{-1}), and (b) 30 nm (50 ng Au L^{-1}). Acquired using a mobile phase flow rate of 1.6 mL min^{-1} . Each contour plot is constructed from its corresponding original spike-chromatogram as described in this article.

14. Replicate injections of the same solution gave 47 ± 11 and 46 ± 10 ions detected per NP, with 62 and 47 NPs detected, respectively. The average from the three analyses was 48 ions detected per NP, with 54 NPs detected. As expected, spike intensity did not change when analyzing 60 nm Au-NP solutions at different metal concentrations, but of course the number of signal spikes detected did so in a linear fashion, as will be discussed in more detail in this article.

A more convenient way to view HDC – SP-ICPMS data and obtain complimentary information is by transforming the spike-chromatograms into contour plots, i.e. as shown in **Figure 3**. In this case the three types of information obtained from the HDC – SP-ICPMS analysis, i.e. retention times, number of signal spikes, and ions counted per 10 ms dwell time, are transformed and presented in the form of a contour plot. In such plots, the presence of Au-containing NPs is observed in the form of a “color map”. This makes it easier to visually observe the presence of NPs having different properties. In **Figure 3** two

separate solutions of 60 nm and 30 nm Au-NPs were analyzed and their resulting spike-chromatograms converted into contour plots (**Figure 3a** and **3b**, respectively).

The transformation procedure followed in order to convert the spike-chromatograms to their corresponding contour plots is described here briefly. The original data consisted of two data columns, one corresponding to dwell time and the other to intensity, i.e. one intensity reading per 10 ms dwell time. Subsequently, intensity bins with a 10 count range were made for each dwell time, i.e. intensity bin (in.bin) #1: 4-10 counts, in.bin #2: 11-20 counts, in.bin #3: 21-30 counts, ..., in.bin #10: 91-100 counts. The first in.bin. starts from 4 counts in order to avoid counting background signals. This resulted in a 9803 (dwell times) x 10 (intensity ranges) data point grid for the acquired 100 s NP-eluting portion of the chromatogram. All intensity bins were initially assigned a zero (0) for all dwell times that were acquired. Only if a signal spike, with an intensity > 4 counts, was detected at a given dwell time was a 1 (one) placed in its corresponding intensity bin. The next and final transformation involved summing the number of NPs detected in each intensity bin for 5 sec time intervals. This gave the final dataset, a 40 x 10 data point grid, used to construct the displayed contour plots.

Analysis of NP mixtures. When analyzing NP mixtures by using HDC – SP-ICPMS the resulting spike-chromatograms become exceedingly complicated and visual inspection does not allow for the unambiguous detection of NPs of different sizes. This difficulty originates both from the nature of the signal spikes (a few early or late eluting NPs can confuse visual evaluation of retention times), and also the fact that HDC is a relatively low resolution separation technique; thus, not completely separating NPs of similar size. To illustrate this, a solution containing a mixture of 30 and 60 nm Au NPs was analyzed using the HDC – SP-ICPMS and the resulting spike-chromatogram is presented in **Figure 4a**. In this case, it is clearly observed that HDC does not have sufficient resolving power to adequately separate these two closely sized NPs. Once again visual inspection of the spike-chromatogram leaves ambiguity regarding the presence of different sized particles. To overcome this, the resulting spike-

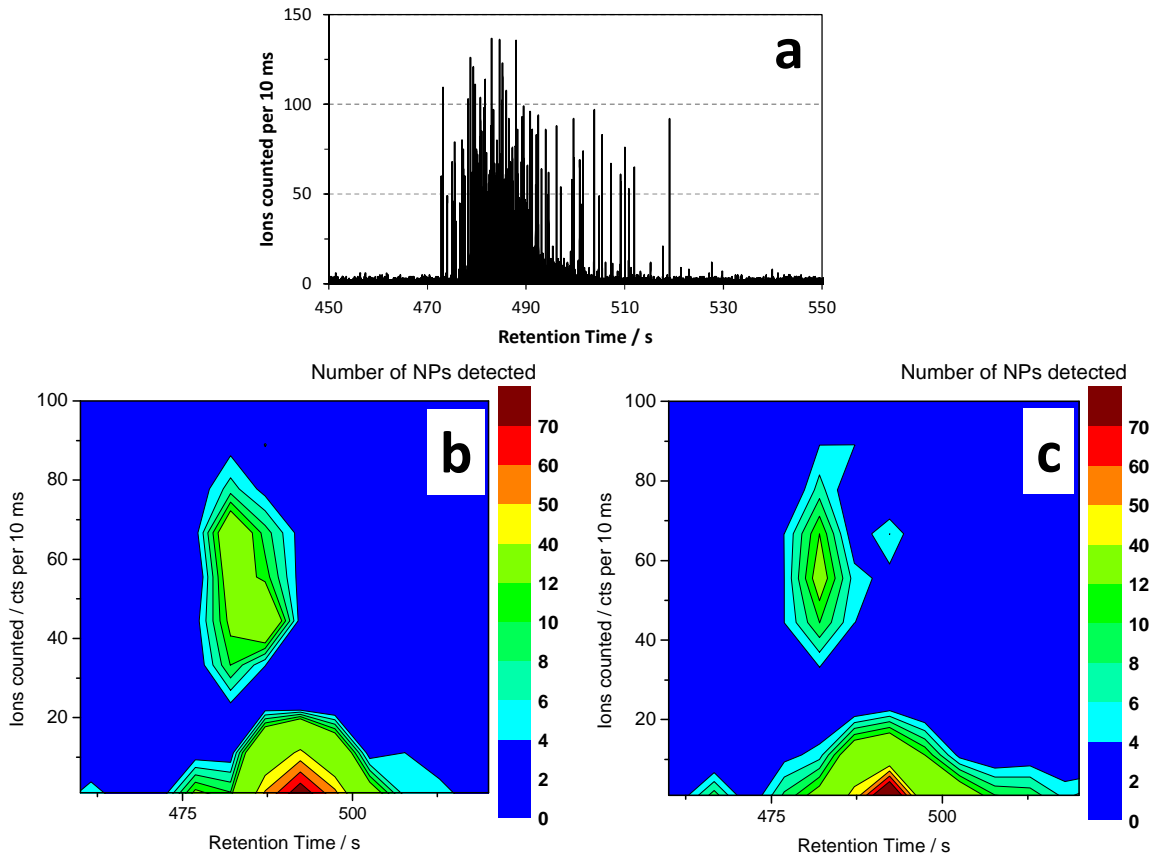


Figure 4 Spike-chromatogram along with contour plots obtained from the HDC – SP - ICPMS analysis of Au-NP mixtures made to contain 60 nm and 30 nm particles in de-ionized water (a and b), and in bottled drinking water (c). The concentration of Au in the form of these two NP sizes is 200 ng Au L⁻¹ and 50 ng Au L⁻¹, respectively. A mobile phase flow rate of 1.6 mL min⁻¹ was used.

chromatogram was transformed, as described previously, to its corresponding contour plot (**Figure 4b**). Here we can clearly observe two different types of NPs, the 60 and 30 nm Au-NPs present in this solution. Thus we observe that the SP-ICPMS approach further enhances the resolving power of this hyphenated system. Similarly, when 60 and 30 nm Au-NPs are spiked into bottled drinking water and analyzed, the resulting contour plot reveals the presence of Au-NPs of two different sizes (**Figure 4b**). Overall, these contour plots enhance our immediate ability to gain a qualitative insight regarding the different types of NP present in our samples.

It should be noted that when analyzing NP mixtures (30 and 60 nm NPs) there exists an increased possibility for co-eluting NPs of both sizes to be counted within the same dwell time thus giving some slightly more intense counts for the 60 nm NPs. In terms of the qualitative interpretation of the resulting contour plots this is not expected to have any great effect, i.e. in fact when comparing **Figure 3a** (60 nm NPs only) with **Figure 4b** (mixture of 60 and 30 nm NPs) only a slight increase in the number of intensity spikes above 80 counts is observed in the latter case. However, it is expected that improved instrumentation will allow for shorter dwell times which in turn will significantly reduce the chance for more than one NP to occur per dwell time, thus allowing for the more efficient analysis of NP mixtures.

HDC – SP-ICPMS for NP Characterization

In the next step of this study we provide proof of principle for the suitability of HDC – SP-ICPMS to determine: (a) NP number concentrations, (b) NP size, and (c) the metal content of individual NPs. To realize these characterization metrics, a procedure employing three calibrations is used. The first calibration correlates the number of NPs detected, i.e. signal spikes counted, to the number of NPs injected. The second calibration correlates NP retention time observed on the HDC column to NP size. Finally, the third calibration correlates the number of ions detected per NP, i.e. spike intensity, to the metal content of individual NPs. To construct these three calibrations it is necessary to conduct two different experiments. The first involves, analyzing several solutions of NPs of well characterized size, e.g. 60 nm Au NPs, in which Au-NPs are present at increasing number concentrations, and counting the

number of resulting signal spikes (Calibration 1). The second calibration experiment involves analyzing solutions of NPs of various sizes, i.e. 26.8, 55.4, 80 and 100 nm, and recording their retention time (Calibration 2) and the average intensity of their corresponding signal spikes (Calibration 3).

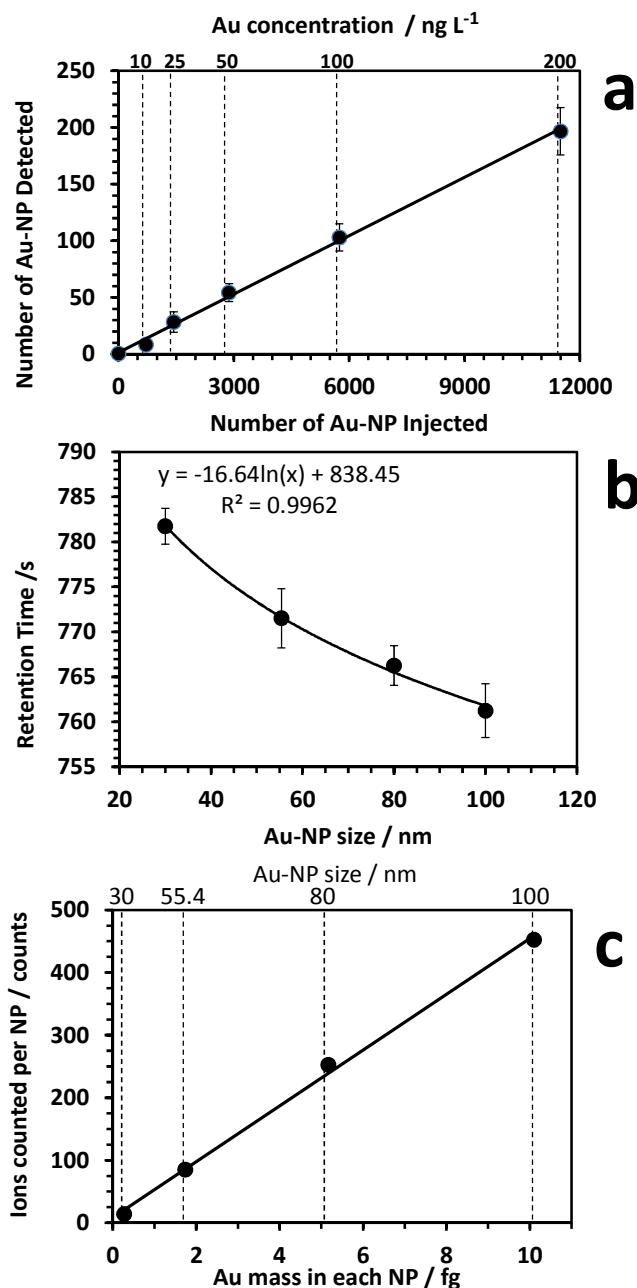


Figure 5 Calibration curves for converting: (a) the number of NPs detected into the number of Au-NPs injected, (b) Au-NP retention time into NP size, and (c) signal spike intensity into Au mass per NP. Flow rate used for these calibrations was 1 mL min⁻¹. Error bars represent ± 1 standard deviation of measured parameter for $n=3$.

Determining NP number concentrations (Calibration 1). When analyzing a series of standard solutions containing 60 nm Au-NPs (NIST RM 8013) at increasing number concentrations, it is observed that the

number of detected signal spikes is linearly proportional to the solution's NP number concentration (**Figure 5a**). Each data point in the calibration plot is the average of a triplicate analysis of the corresponding Au-NP standard. Linear regression analysis gave equations such as: $Y_{(\# \text{ NPs Detected})} = 0.0172 X_{(\# \text{ NPs Injected})} + 1.371$; $R^2 = 0.9978$, for both 60 and 30 nm Au NPs. Such equations can be used to determine Au-NP number concentrations in unknown samples from the number of signal-spikes detected during their analysis. The equation slope is a measure of the transport efficiency for the analyzed Au-NPs. The transport efficiency for the system used in this study, which included using a V-groove nebulizer and a double pass Scott spray chamber, was found to be approximately 1.7%. A recent study has described in detail alternative approaches for determining transport efficiency for SP-ICPMS analysis.³¹ Such approaches can also be used for the hyphenated system described here. The limit of detection for 60 nm Au-NP solutions was calculated from the calibration curve to be 600 Au-NP per mL of sample or 60 Au-NP injected in a 100- μ L injection volume. This would correspond to a Au concentration LOD of 2.2 ng Au L⁻¹.

The 60 nm Au-NP solutions used here, i.e. NIST RM 8013, have been certified for their concentration in Au and also for their Au-NP size. It has also been shown that these NPs are spherical in shape. Taking this information into account and using the density of Au and a reference material solution density of 1 g mL⁻¹ it is possible to calculate the Au-NP number concentration present in NIST RM 8013 solution. Knowing the NP number concentration of the stock solution, appropriate dilutions were made for calibration standards of known Au-NP number concentration (**Figure 5a**), ranging from approximately 5×10^3 to 11×10^4 NPs mL⁻¹. Using NP number concentrations greater than the upper limit of our calibration would result in an increased possibility of having multiple NPs enter the plasma per 10 ms dwell time, thus further confounding the analysis and negating an important requirement of SP-ICPMS (i.e., ≤ 1 NP detected per dwell time).

NP size determination (Calibration 2). Size calibration of the HDC separation is achieved by recording the retention times (t_R) of a series of different sized Au-NP standards and plotting them as a function of

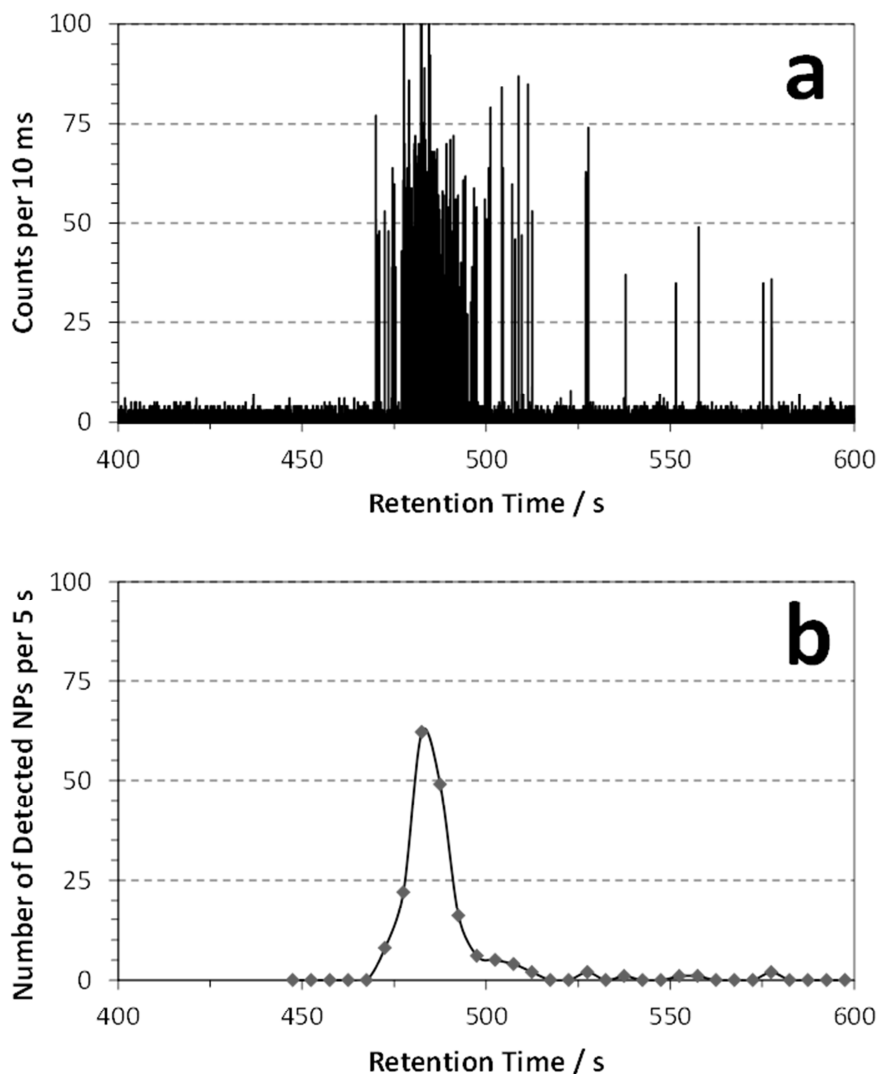


Figure 6 HDC – spICPMS chromatograms acquired following the analysis of a solution containing 60 nm Au-NPs at a concentration of 200 ng Au L⁻¹. Acquired at mobile phase flow rate of 1.6 mL min⁻¹. Original spike chromatogram without any data processing (a), and processed chromatogram in which the number of signal spikes detected per 5 s time windows have been summed and plotted as a function of average retention time (b). The latter process allows for the viewing of the spike chromatogram as a conventional chromatogram. In addition, retention time determination is more convenient.

NP size (**Figure 5b**). However, extracting the retention time from a spike-chromatogram is not as straightforward as obtaining it from a conventional chromatographic peak where its apex is clearly identifiable and assigned to be the analytes t_R . In the spike chromatogram the maximum detection frequency of signal spikes would correspond to its number concentration apex. However, this is not always a straightforward procedure as t_R accuracy and precision would depend on the time window used

to count the signal spikes. To overcome this difficulty two procedures were evaluated. First, t_R assignment was made after reconstructing a conventional chromatogram from the recorded spike-chromatogram shown in **Figure 6a**. This is achieved by summing the number of signal spikes observed during a 5 sec time window (5 s bin) and plotting these sums as a function of its average retention time (**Figure 6b**). The retention time of the resulting chromatographic peak can be conveniently assigned this way, however, it will be associated with an uncertainty dictated by the size of the applied time bin, i.e. time bin of 5 s in this case and thus ± 2.5 s. An alternative statistical approach would be to record the t_R of all the detected Au-NPs of given size, i.e. t_R of all signal spikes of a given intensity. Subsequently their average t_R is calculated and assigned to be their retention time.

The relationship between NP retention time and size, as determined for the Au-NPs analyzed on our system using the latter approach, is described by the equation $Y_{(\text{NP retention time})} = -16.64 \text{ Ln}(X_{\text{NP size}}) + 838.45$; $R^2=0.9962$ (**Figure 5b**). Such an equation can be used to determine NP size in unknown samples from their retention times. In a previous study,¹⁹ the relationship between Au-NP size and their retention time was also found to be logarithmic for NPs ranging from 5 nm to 250 nm in diameter.

Overall, however, it is our view that the accuracy with which size calibration can be achieved using HDC for nanosized particles is one of the fundamental limitations of the HDC – SP-ICPMS approach. This is because even small retention time shifts, if not corrected for, will introduce substantial uncertainty into NP size determination.

Determining the metal mass fraction of NPs (Calibration 3). The counting statistics of the ICPMS detector and NP size inhomogeneity account for the intensity variations observed for the individual signal spikes (**Figure 2** and **6**). However, it is also well known from SP-ICPMS analysis that the average intensity observed for each detected spike is proportional to the mass of Au present in that particular NP. Various procedures have so far been proposed for converting the average spike intensity into metal mass fraction of each NP.^{25-27, 31} Here we have used an alternative approach which uses the calibration data acquired from the NP-size calibration, whereby the mass of Au in each of the

calibration Au-NPs is related to the average intensity of the signal spikes (**Figure 5c**). The mass of Au in each of the Au-NP sizes is calculated by knowing their diameter, observing that they are approximately spherical by TEM and SEM, and that they only contain Au. Au-NPs of different sizes each give spike signals of different intensity. By plotting signal spike intensity as a function of Au mass per NP (**Figure 5c**) the following linear relationship is observed: $Y_{(\text{ions detected per single NP})} = 44.62 X_{(\text{fg of Au per single NP})} + 8.35$; $R^2=0.9977$. Such a calibration allows for the conversion of the observed signal spike intensity to metal mass per single NP.

As already mentioned in the present study, but also demonstrated in previous studies, SP-ICPMS without any chromatography can be used for the determination of the metal mass fraction of NPs by analyzing a standard solution of the metal in its dissolved form, i.e. Au in this case, along with the Au-NPs.²⁷ We have therefore also evaluated this approach in combination with HDC. When analyzing the NIST RM 8013, Au-NPs with a nominal size of 60 nm, we determined them to have a diameter of 56.3 nm. This compares well with the average 55.4 nm obtained by NIST using several independent analytical techniques. Details of our single particle calculations are provided in the Supporting Information section of this paper.

Determining Au-NP size, number concentration and Au mass fraction. By using all three calibrations it is possible to convert non-calibrated contour plots such as the ones already presented (**Figures 4**) into calibrated contour plots showing Au-NP size, Au mass fraction and Au-NP number concentrations. Such a procedure was carried out for a bottled drinking water sample spiked to contain 60 nm and 30 nm Au-NPs. The resulting calibrated contour plot is shown in **Figure 7**. In this plot it is easy to observe that two different types of Au-NPs are present. One being between 10-30 nm in size, with each NP containing approximately 0.15-0.3 fg of Au. Also, by summing the number of this type of Au-NPs from the calibrated grid, i.e. summed the number of NPs present in appropriate time and intensity bins, a total of 18363 Au-NPs between the size of 10-30 nm were detected. In fact based on calculations using data provided by NIST for RM 8012 (see Materials experimental section) we would expect this sample to

contain Au-NPs of 26.8 (with NIST reported values from 24.6 to 28.6 nm), each having a Au mass fraction of 0.27 fg. Also, as these NPs had been spiked into the bottled drinking water at a concentration of 50 ng Au L⁻¹, the number of NPs expected to be present was 18518; therefore, a 99% recovery was achieved.

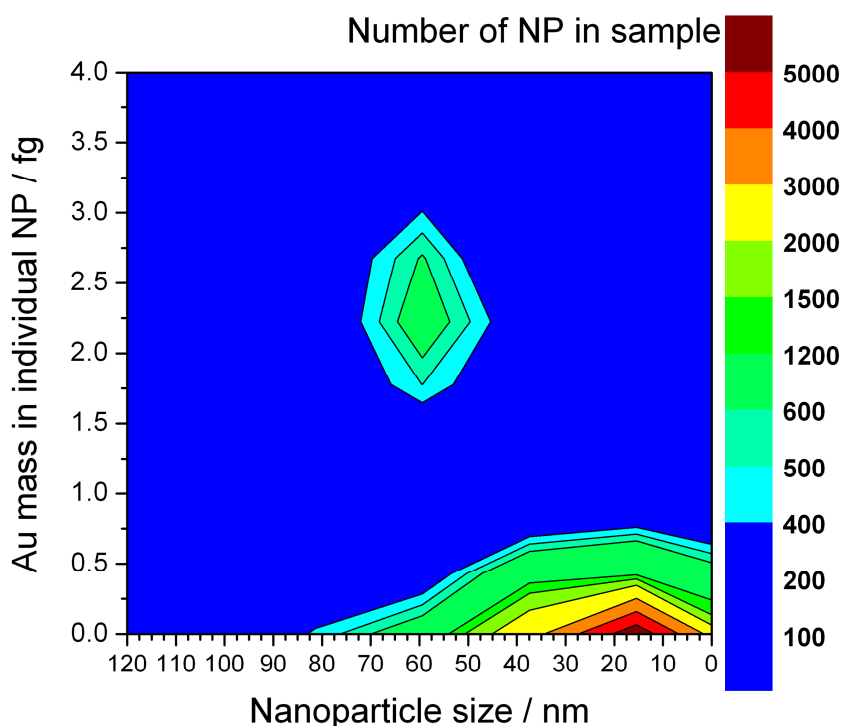


Figure 7 Calibrated contour plot showing the analysis of a drinking water sample spiked with NIST RMs having nominal sizes of 60 and 30 nm, at concentrations of 100 and 50 ng Au L⁻¹, respectively.

The second type of detected Au-NPs appear in the calibrated contour plot to have a size of 55-65 nm, with each NP containing between 2.0 and 2.5 fg of Au. Based on calculations using data provided by NIST for RM 8013 (see Materials experimental section) we would expect 1.74 fg of Au per NP, and a size of 55.4 ± 1.1 nm. Also, as these NPs had been spiked into the bottled drinking water at a concentration of 100 ng Au L⁻¹ the number of NPs expected to be present was 5747, whereas 3936 were detected, thus a 68% recovery was achieved. Thus, indicating interaction with the water matrix or poor column recovery.

Technical difficulties encountered developing and using the HDC – SP-ICPMS approach. Several technical challenges were encountered during the development of this technique. The first involved the occurrence of random background signal-spikes at m/z 197 when a reciprocating piston liquid chromatography pump was initially used instead of the syringe pump adopted later. After further investigation it was concluded that metal-containing particles were coming off the piston pump during its operation. After further investigation it was observed that high intensity signal spikes were observed for m/z 181 when the piston pump was connected directly to the SP-ICPMS. This mass corresponds to monoisotopic tantalum (Ta) which is an element known to form oxide polyatomic ions with a m/z of 197. The average intensity of the m/z 197 background spikes to those observed at m/z 181 indicate a 1-2% TaO^+ level relative to Ta^+ . Following this observation, the reciprocating piston pump was replaced by a syringe pump, in which case the previously observed background spikes at m/z 197 and 181 were no longer observed.

The second technical difficulty we encountered was the ICPMS limitation of 10 ms being the lowest possible dwell time per m/z when monitoring a single isotope. In the single particle mode it is desirable to use even lower dwell times in order to minimize the possibility of having two or more Au-NPs measured within the same dwell time. Another instrument feature that posed a significant problem was the delay with which a 10 ms data point for a single m/z was downloaded from the instrument to the computer. This delay was significant as it increased analysis time by a factor of 5-6. Therefore, a 10 min chromatographic run required about 50-60 min for all the acquired data to be downloaded. Only after the data had been downloaded could a subsequent run be initiated. The observation of such a data acquisition delay has previously been reported by others, in which case they reported a low data transfer rate of 40 ms per data point.⁴² For both of these limitations no adequate solution was obtained for the duration of this study.

Finally, the fact that SP-ICPMS is such a sensitive technique, i.e. it can detect single particles, precluded the injection of Au-NP solutions containing Au at $\mu\text{g L}^{-1}$ (ppb) levels. The reason for this is that NP contamination can occur resulting in the late elution of few NPs, past their expected retention

time. This creates some visual confusion with respect to the spike-chromatogram. To overcome this problem we used two HDC columns independently in this study, one for $\geq \mu\text{g Au L}^{-1}$ concentrations with conventional mode – ICPMS, mainly for screening purposes, and a second column operated in the ng Au L^{-1} concentration regime with SP-ICPMS. The latter column was used for most of the experiments reported in this study.

Conclusions

Overall, our effort to develop an HDC – SP-ICPMS approach for NP characterization has built substantially on the exceptional preceding studies demonstrating the separate use of HDC and SP-ICPMS for NP determination. In doing so we have described their individual limitations as well as demonstrated their complementarities which was the driving force for our investigating their on-line coupling.

It is concluded that the strong points of the hyphenated approach for NP characterization is its extremely high sensitivity and selectivity, as well as the NP size and number concentration information it is capable of providing. However, it is also apparent that separation methods with higher resolving power are needed for analysis of suspensions of NPs of narrow size distribution. Improved ICPMS sensitivity will allow for the detection of even smaller sized NPs in the single particle mode.

Finally, new software developments will be required for more efficient and convenient data acquisition and processing of the resulting chromatographic and single particle counting data.

NOTICE: The United States Environmental Protection Agency through its Office of Research and Development funded and managed the research described here. It has been subjected to the Agency's administrative review and approved for publication. Mention of trade names or commercial products does not constitute endorsement or recommendation for use.

Acknowledgments: This research was performed while S.A.P held a National Research Council Senior Research Associateship Award at the U.S. Environmental Protection Agency, National Exposure Research Laboratory in Las Vegas, NV.

REFERENCES

-
- ¹ Ponder, S.M.; Darab, J. G.; Bucher, J. M.; Caulder, D.; Craig, I.; Davis, L.; Edelman, N.; Lukens, W. W.; Nitsche, H.; Rao, L.; Shuh, D. K.; Mallouk, T. E. *Chem. Mater.* **2001**, 13 (2), 479-486.
- ² Chaudhry, Q.; Scotter, M.; Blackburn, J.; Ross, B.; Boxall, A.; Castle, L.; Aitken, R.; Watkins, R. *Food Additive Contaminants J.*, 2008, 25 (3), 241-258.
- ³ Rejeski, D. *Nanotechnology and Consumer Products, Consumer Product Safety Commission Hearing*, **2009**. http://www.nanotechproject.org/process/assets/files/8278/pen_submission_cpsc.pdf (accessed Dec. 2011).
- ⁴ Benn, T.M.; Westerhoff, P. *Environ. Sci. Technol.* **2008**, 42 (11), 4133-4139.
- ⁵ Luoma, S.N. *Project on Emerging Nanotechnologies 15 - Silver Nanotechnologies and the Environment*, **2008**, <http://www.nanotechproject.org/publications/archive/silver/> (accessed Dec. 2011).
- ⁶ Geranio, L.; Heuberger, M.; Nowack, B. *Environ. Sci. Technol.* **2009**, 43 (21), 8113-8118.
- ⁷ *Project on Emerging Nanotechnologies, Consumer Products*, **2010**. <http://www.nanotechproject.org/inventories/consumer> (accessed Dec. 2011).
- ⁸ U.S. Environmental Protection Agency, Office of Research and Development, "Nanomaterial Research Strategy". EPA 620/K-09/011, **2009**.
- ⁹ Morris, J.; Willis, J. U.S. Environmental Protection Agency, Nanotechnology White Paper; U.S. Environmental Protection Agency: Washington, DC, February, **2007**.
- ¹⁰ Lin, W.-C.; Yang, M.-C. *Macromolecular Rapid Communications* **2005**, 26 (24), 1942-1947.
- ¹¹ Pyrz, W.D.; Buttrey, D.J. *Langmuir* **2008**, 24 (20), 11350-11360.
- ¹² Ebenstein, Y.; Nahum, E.; Banin, U. *Nano Letters* **2002**, 2 (9), 945-950.
- ¹³ Filella, M.; Zhang, J.; Newman, M.E.; Buffle, J. *Colloids and Surfaces A: Physicochem. Eng. Aspects* **1997**, 120 (1-3), 27-46.
- ¹⁴ Kammer, F. v d; Baborowski, M.; Friese, K. *Anal. Chim. Acta* **2005**, 552 (1-2), 166-174.
- ¹⁵ MacCuspie, R.I.; Rogers, K.; Patra, M.; Suo, Z.; Allen, A.J.; Martin, M.N.; Hackley, V.A. *J. Environ. Monit.* **2011**, 13, 1212-1226.
- ¹⁶ Leshner, E.K.; Ranville, J.F.; Honeyman, B.D. *Environ. Sci. Technol.* **2009**, 43 (14), 5403-5409.
- ¹⁷ Liu, F.-K.; Lin, Y.-Y. Wu, C.-H. *Anal. Chim. Acta* **2005**, 528 (2), 249-254.
- ¹⁸ Pease, III, L.F.; Tsai, D.-H.; Brorson, K.A.; Guha, S.; Zachariah, M.R.; Tarlov, M.J. *Anal. Chem.* **2011**, 83, 1753.
- ¹⁹ Tiede, K.; Boxall, A.B.A.; Tiede, D.; Tear, S.P.; David, H.; Lewis, J. *Anal. Atom. Spectrom.* **2009**, 24, 964-972.
- ²⁰ Hassellöv, M.; Lyvén, B.; Beckett, R. *Environ. Sci. Technol.* **1999**, 33 (24), 4528-4531.
- ²¹ Badawy, A. M. E.; Luxton, T. P.; Silva, R. G.; Scheckel, K. G.; Suidan, M. T.; Tolaymat, T. M. *Environ. Sci. Technol.* **2010**, 44 (4), 1260-1266.
- ²² Handy, R.; Owen, R.; Valsami-Jones, E. *Ecotoxicology* **2008**, 17 (5), 315-325.
- ²³ Tiede, K., Boxall, A. B. A.; Tear, S. P.; Lewis, J.; David, H.; Hassellöv, M. *Food Additives & Contaminants. Part A: Chemistry, Analysis, Control, Exposure & Risk Assessment* **2008**, 25 (7), 795-821.
- ²⁴ Tiede, K.; Boxall, A.B.A.; Wang, X.M.; Gore, D.; Tiede, D.; Baxter, M.; David, H.; Tear, S.P.; Lewis, J. *J. Anal. Atom. Spectrom.* **2010**, 25, 1149-1154.
- ²⁵ Degueldre, C.; Favarger, P.-Y.; Bitea, C. *Anal. Chim. Acta* **2004**, 518, 137-142.
- ²⁶ Degueldre, C.; Favarger, P.-Y. *Talanta* **2004**, 62, 1051-1054.
- ²⁷ Degueldre, C.; Favarger, P.-Y.; Wold, S. *Anal. Chim. Acta* **2006**, 555, 263-268.
- ²⁸ Monserud, J.H.; Leshner, E.K.; Ranville, J.F. *237th ACS National Meeting*, Salt Lake City, Utah, **2009**.
- ²⁹ Mitrano, D.M.; Barber, A.; Bednar, A.; Westerhoff, P.; Higgins, C.P.; Ranville J.F. *J. Anal. Atom. Spectrom.* **2012**, 27, 1131-1142.
- ³⁰ Olesik, J.W.; Gray, P.J. *J. Anal. Atom. Spectrom.* **2012**, 27, 1143-1155.
- ³¹ Pace, H.E.; Rogers, N.J.; Jarolimek, C.; Coleman, V.A.; Higgins, C.P.; Ranville, J.F. *Anal. Chem.* **2011**, 83 (24), 9361-9369.

-
- ³² Nomizu, T.; Hayashi, H.; Hoshino, N.; Tanaka, T.; Kawaguchi, H.; Kitagawa, K.; Kaneco, S. *J. Anal. Atom. Spectrom.* **2002**, *17*, 592-595.
- ³³ Nomizu, T.; Nakashima, H.; Hotta, Y.; Tanaka, T.; Kawaguchi, H. *Anal. Sci.* **1992**, *8*, 527-531.
- ³⁴ Hassellöv, M. *Setac Europe*, Goteborg, **2009**.
- ³⁵ Kapellios, E.A.; Pergantis, S.A. *J. Anal. Atom. Spectrom.* **2012**, *27*, 21-24.
- ³⁶ NIST Reference Material 8013, Gold Nanoparticles nominal 60 nm diameter, Report of Investigation. <http://www.nist.gov/srm/index.cfm>
- ³⁷ NIST Reference Material 8012, Gold Nanoparticles nominal 30 nm diameter, Report of Investigation. <http://www.nist.gov/srm/index.cfm>
- ³⁸ Yegin, B. A.; Lamprecht, A. *Int. J. Pharm.* **2006**, *320*, 165.
- ³⁹ Stewart, I.I.; Olesik, J.W. *J. Am. Soc. Mass Spectrom.*, **1999**, *10*, 159-174.
- ⁴⁰ Heithmar, E. M. *237th ACS National Meeting*, Salt Lake City, Utah, **2009**.
- ⁴¹ Degueldre, C.; Favarger, P.-Y. *Colloids and Surfaces A: Physicochem. Eng. Aspects* **2003**, *217*, 137-142.
- ⁴² Ho, K.-S.; Chan, W.-T. *J. Anal. Atom. Spectrom.* **2010**, *25*, 1114-1122.

For TOC only:

